Monthly Notices
of the
ROYAL ASTRONOMICAL SOCIETY

Mon. Not. R. Astron. Soc. **410,** 1496–1502 (2011) doi:10.1111/j.1365-2966.2010.17534.x

Constraining the molecular gas in the environs of a $z \sim 8$ gamma-ray burst host galaxy

Elizabeth R. Stanway,[1⋆] Malcolm N. Bremer,[1] Nial R. Tanvir,[2] Andrew J. Levan[3] and Luke J. M. Davies[1]

[1]*H. H. Wills Physics Laboratory, Tyndall Avenue, Bristol BS8 1TL*
[2]*Department of Physics and Astronomy, University of Leicester, University Road, Leicester LE1 7RH*
[3]*Department of Physics, University of Warwick, Coventry CV4 7AL*

Accepted 2010 August 15. Received 2010 August 6; in original form 2010 June 7

ABSTRACT

GRB 090423 is the most distant spectroscopically confirmed source observed in the Universe. Using observations at 37.5 GHz, we place constraints on molecular gas emission in the CO (3–2) line from its host galaxy and immediate environs. The source was not detected either in line emission or in the rest-frame 850-μm continuum, yielding an upper limit of $S_{8\mathrm{mm}} = 9.3\,\mu\mathrm{Jy}$ and $\mathrm{M(H_2)} < 4.3 \times 10^9\,\mathrm{M}_\odot$ (3σ), applying standard conversions. This implies that the host galaxy of GRB 090423 did not possess a large reservoir of warm molecular gas but was rather modest either in star formation rate or in mass. It suggests that this was not an extreme starburst and hence that gamma ray bursts at high redshift trace relatively modest star formation rates, in keeping with the behaviour seen at lower redshifts. We do, however, identify a millimetre emission-line source in the field of GRB 090423. Plausible interpretations include a CO (1–0) emitting galaxy at $z = 2.1$, CO (2–1) at $z = 5.2$ and CO (3–2) at $z = 8.3$. Efforts to identify a counterpart for the molecular line emitter and to further characterize this source are continuing.

Key words: gamma-ray burst: individual: GRB 090426 – galaxies: high-redshift – radio lines: galaxies.

1 INTRODUCTION

Gamma ray bursts (GRBs) are amongst the most useful probes of the early Universe. Their utility is twofold, both in yielding information about their host galaxy and immediate environment and as beacons, marking out mass and structure at the highest redshifts (Lamb & Reichart 2000). Given their high energies, they can potentially be observed out to $z = 15$ or further with current instruments, but redshift determination for these high-redshift bursts is challenging, requiring deep integrations with optical and near-infrared telescopes in the hours after a source is detected. Despite this, the few known $z > 5$ sources have provided valuable evidence for the properties of dust (Stratta et al. 2007) and molecular clouds (Campana et al. 2007) at these early times and for the column density of neutral hydrogen in their environment (Totani et al. 2006; Ruiz-Velasco et al. 2007).

While GRBs do not require massive host galaxies (Savaglio, Glazebrook & LeBorgne 2009; Svensson et al. 2010), they do require the presence of significant quantities of gravitationally collapsed and processed baryonic matter in the form of young stars. At high redshifts, this condition is believed to be sufficiently rare to make them likely markers of overdense regions in the cosmic web and hence a measure of the power of small-scale density fluctuations (Mesinger, Perna & Haiman 2005). Using such beacons may be the only way to identify and characterize star-forming regions during cosmic reionization – the epoch during which the first stars heated and ionized neutral hydrogen atoms in the intergalactic medium.

GRB 090423 at $z = 8.23^{+0.06}_{-0.07}$ is the most distant known object with a well-defined, spectroscopically confirmed redshift (Salvaterra et al. 2009; Tanvir et al. 2009). Occurring just 600 Myr after the big bang, it likely probes the tail end of the epoch of reionization. Its afterglow and host galaxy provide an unprecedented opportunity to probe the properties of a star-forming galaxy at these early times, and it is likely to be the archetype for future observations on similarly distant GRBs [see the Decadal Survey Whitepaper by McQuinn et al. (2009) for discussion].

Crucially, the properties of GRB 090423 are consistent with the bulk of the GRB population (Tanvir et al. 2009), lacking the long duration and extreme energy output that might be expected from a Pop III progenitor (Mészáros & Rees 2010). As such, this burst must mark out a region in which star formation is already well underway and in which the interstellar and intergalactic media have already undergone processing. For this to have occurred at such

⋆E-mail: e.r.stanway@Bristol.ac.uk

high redshifts requires this region to have collapsed early in the history of the Universe, implying that it is highly overdense relative to the volume average at early times. By $z = 8$, it is possible for dark matter haloes as massive as a few 10^{12} $M_\odot$ to have collapsed, albeit in small numbers (Mo & White 2002). While GRB 090423 is not coincident with a known active galactic nucleus (AGN), it could plausibly lie either in a massive halo or in the mass overdensity associated with such a halo.

Interpretation of high-redshift bursts, particularly in the context of evolutionary trends such as the cosmic star formation rate history and inferences made from it (e.g. Kistler et al. 2009; Wang & Dai 2009; Wyithe et al. 2010), requires an understanding of the burst environment and how it too changes with redshift. At low redshift, GRBs are not unbiased tracers of star formation but are seen to occur preferentially in low-mass, metal-poor galaxies (Savaglio et al. 2009; Svensson et al. 2010). Semi-analytic models, applied to large simulations such as the Millennium Simulation, suggest that GRB host galaxy halo mass is largely independent of redshift to $z > 6$ (Chisari, Tissera & Pellizza 2010), but observational evidence for this is sparse. Kistler et al. (2009) have suggested that the ratio of the GRB rate to star formation density scales as $(1+z)^{1.2}$, possibly due to evolution in the mean metallicity. If host galaxy stellar masses, star formation rates or dark matter halo masses (and hence clustering) of GRB hosts evolve with redshift, then the interpretation of burst rate as a proxy for star formation rate history will need to be revisited and refined.

GRB 090423 provides a case study at high redshifts, potentially probing significant evolution in environment from $z < 1$ burst hosts. Given that the GRB appears to be the result of a second generation or later starburst at such early times, does it occupy a more massive galaxy than typical of lower redshift bursts, a vigourous starburst, a mature system that has exhausted its gas supply or a young one with a large reservoir of processed molecular gas available for later star formation?

One test of the latter hypothesis has become possible due to the broad bandwidth and high sensitivity of the current generation of millimetre telescopes. At $z = 8$, the rest-frame infrared CO (3–2) emission line (a good probe of molecular gas mass at low redshift) is shifted into the observed 7-mm band. The 4-GHz bandwidth available using the new CABB correlator at the Australia Telescope Compact Array (ATCA) enables a volume with line-of-sight extent $\Delta z = 0.9$ to be observed in a single observation, easily encompassing the redshift uncertainty from optical/near-infrared observations. Given the high redshift of this and similar sources, carbon monoxide and other far-infrared emission lines (notably [C II] at 1898 GHz) may well prove the most accessible diagnostics of the precise redshift of the GRB host and any galaxies sharing a large-scale structure surrounding it.

In this paper, we describe an investigation to study the CO (3–2) emission-line properties of the GRB host galaxy and neighbouring galaxies in its immediate environs. We structure the paper as follows. In Section 2 we describe our observations, targeted on the host galaxy of GRB 090423 and searching for CO (3–2) emission. In Section 3, we present limits obtained on the properties of the GRB host. In Sections 4.1 and 4.2, we present the properties of additional sources detected in our data, first in continuum and then in molecular line emission. Finally, in Section 5, we discuss the interpretation and implications of our results, before presenting our conclusions in Section 6.

All optical and near-infrared magnitudes in this paper are quoted in the AB system (Oke & Gunn 1983). We adopt a Λ cold dark matter cosmology with $(\Omega_\Lambda,\ \Omega_M, h) = (0.7, 0.3, 0.7)$.

2 OBSERVATIONS

Observations were carried out over the period from 2010 March 22 to 26, using the 7-mm band receivers at the ATCA.[1] The 4-GHz bandwidth CABB correlator was used, with a small overlap between the two intermediate frequencies, allowing continuous frequency coverage in the range of 36.075–39.723 GHz, at 1-MHz resolution. A single pointing was observed at $09^h55^m33\overset{s}{.}29+18^\circ08'50\overset{''}{.}80$, placing the GRB host galaxy 10 arcsec north of the phase centre. The primary beam full width at half-maximum (FWHM) of the ATCA at 38 GHz is 75 arcsec.

GRB 090423 is well north of the optimal declination for the ATCA. As a result, observations were split into five tracks and the source was observed at elevations of $> 30^\circ$ for 4.9 h per track. To ensure good uv coverage and sensitivity at millimetre wavelengths, observations were taken in the compact H168 configuration, yielding a typical synthesized beam of 7.8×6.3 arcsec^2 at half-power beamwidth.

Bandpass calibration was performed on PKS 0537−441 at the start of every track, and nearby phase calibrator PKS 0953+254 was observed at 10–15 min intervals throughout the observations. The same source was used to check the array pointing solution once an hour. PKS 1934−638 (the standard flux calibrator at the ATCA) was observed at the end of every track to provide primary flux calibration.

Observations were scheduled at night in order to obtain the most stable possible conditions for 7-mm band observations. Conditions were generally good throughout the observations, but data taken at elevations of $< 30^\circ$ were discarded due to a combination of increased atmospheric opacity and less stable conditions at the start and end of each night. Images were generated using natural weighting. The measured rms noise at the phase centre in the final images was typically 74 μJy beam^{-1} at 37 GHz and 78 μJy beam^{-1} at 39 GHz in 2-MHz (16 km s^{-1}) channels.

A multifrequency (4-GHz bandwidth) synthesis image centred at 37.887 GHz was also generated from the data, reaching a sensitivity limit (rms) of 3.1 μJy beam^{-1}.

3 CONSTRAINTS ON THE $z \sim 8$ GRB HOST

The position of the $z \sim 8$ GRB 090423 is known to sub-arcsecond accuracy (from near-infrared imaging of the burst afterglow). The stellar light from galaxies at these distances is believed to have a typical half-light radius of ∼0.3 kpc (0.06 arcsec), based on photometrically selected samples (Oesch et al. 2010). The beam size of our ATCA observations is two orders of magnitude greater than this, and any emission from the GRB host galaxy itself is likely to be contained within a synthesized beam centred at the burst location (and probing a region 40×30 kpc^2 in extent). Our initial analysis focused on the properties of our data at this location.

No continuum source was seen at the GRB location in the multifrequency synthesis image, allowing us to place an upper limit on the 37.9-GHz continuum flux of this source of $S_{8\mathrm{mm}} = 9.3$ μJy (3σ, assuming the source is unresolved). This observed frequency corresponds to the rest-frame 850-μm band and so probes the warm dust in the system. We use the prescription of Aravena et al. (2008) to calculate an upper limit on the dust mass at $z = 8.2$, assuming that the dust emission can be modelled by a modified blackbody and

[1] Observations associated with programme C2153-2009OCTS.

accounting for the heating effect of the cosmic microwave background at this redshift. A number of significant assumptions are required to make this calculation. Most crucially, the dust coefficient and emissivity index are fixed at local values, which may not be appropriate for high-redshift sources, particularly young and unevolved sources which are likely to be dominated by supernova-processed dust grains (see Maiolino et al. 2004; Stratta et al. 2007). There is also a weak dependence on the assumed size of the source. In the absence of further data, we assume a source extent of 1 kpc, while noting that increasing this by an order of magnitude has negligible effect on the derived mass.

Our derived upper limit on the dust mass in this source is $8.0 \times 10^8\,\mathrm{M}_\odot$ at 40 K. Given the typical stellar masses of GRB host galaxies at low redshift (see Section 5), our non-detection of the source in dust continuum is unsurprising. The mean 850-μm (observed) flux measured by Tanvir et al. (2004) for a sample of 21 GRB hosts at $0.45 < z < 3.42$ implies an average dust mass of only $\sim 5 \times 10^7\,\mathrm{M}_\odot$ for the lower redshift GRB host population using the same prescription applied here. For thermal dust emission across a reasonable range of temperatures, and for a typical low-redshift GRB host galaxy, our constraint implies only that the dust mass does not exceed the stellar mass.

In addition to probing the dust continuum of the source, our observations are sensitive to CO (3–2) line emission spanning the redshift range $7.7 < z < 8.6$ – easily encompassing the $\Delta z = 0.13$ uncertainty in the optical redshift estimate for the GRB host. We have examined our data cube carefully for such emission. Low luminosity galaxies at high redshift have been observed to have lower linewidths than most submillimetre galaxies. Indeed, the only two known $z \sim 5$, non-AGN, CO-emitting galaxies have linewidths of $\sim 160\,\mathrm{km\,s^{-1}}$ (Coppin et al. 2010) and $\sim 110\,\mathrm{km\,s^{-1}}$ (Stanway et al. 2008), respectively, which may suggest that the molecular gas in these sources does not form a rotationally supported disc. With these narrow lines in mind as a model, we select $150\,\mathrm{km\,s^{-1}}$ as a plausible velocity width for any emission line in our distant source.

In order to optimize our sensitivity to emission with this and a variety of both broader and narrower velocity widths, the spectral data cube was rebinned at resolutions of 2, 4, 8 and 16 MHz and each rebinned cube was analysed independently. Despite this, a spectrum taken through the data cube at the location of the GRB host galaxy shows no evidence for line emission at the sensitivity limit of the data at any spectral resolution (see Fig. 1). This places an upper limit on the velocity-integrated linewidth of the CO (3–2) transition (expected at $37.45^{+0.29}_{-0.24}$ GHz) of $S_{\mathrm{CO}}\Delta v < 0.026\,\mathrm{Jy\,km\,s^{-1}}$ (3σ) for a $150\,\mathrm{km\,s^{-1}}$ wide emission line.

The estimation of molecular gas mass from CO line intensity requires the application of an empirical calibration for $\mathrm{M_{gas}}/L'_{\mathrm{CO}}$. For ease of comparison with other authors, we assume that the molecular gas in this source is optically thick and apply the standard conversion factor $\mathrm{M_{gas}}/L'_{\mathrm{CO}} = 0.8\,\mathrm{M}_\odot\,(\mathrm{K\,km\,s^{-1}})^{-1}$, derived for ULIRGs and SMGs at intermediate redshifts and believed to be constant for such sources between $z = 0$ and 4 (see Solomon & Vanden Bout 2005). Using this conversion, we determine an upper limit on the molecular gas at $z = 8.23$ of $\mathrm{M(H_2)} < 4.3 \times 10^9\,\mathrm{M}_\odot$ (3σ).

We note that the conversion has not yet been demonstrated for low-mass galaxies forming stars at a relatively low rate, at significantly sub-solar metallicities or at early times, for which a higher conversion factor may be more appropriate. Applying the Galactic conversion factor, $\mathrm{M_{gas}}/L'_{\mathrm{CO}} = 4.6\,\mathrm{M}_\odot\,(\mathrm{K\,km\,s^{-1}})^{-1}$, would yield limits which are a factor of 5.75 times weaker than those presented here. The true value of the conversion factor is unknown but likely to lie somewhere between these extremes (see discussion in Tacconi et al. 2008).

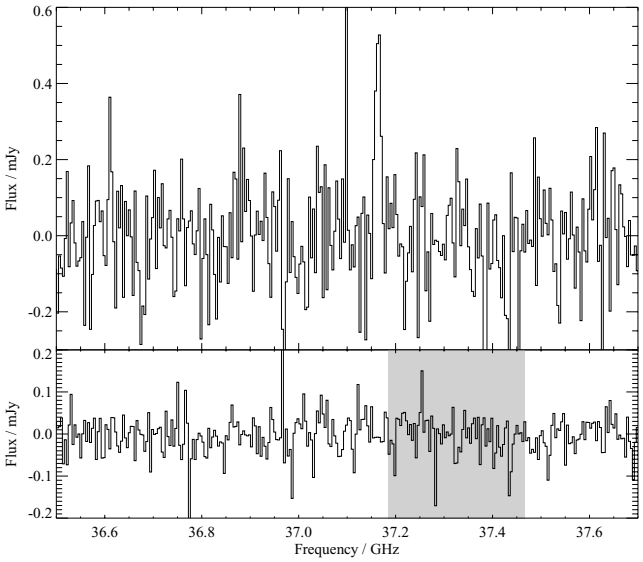

Figure 1. The spectrum of our emission-line source (top panel: see Section 4.2), compared with the non-detection spectrum extracted at the location of the GRB host galaxy (bottom panel: see Section 3) and assuming that the latter is a point source. Data are binned to 4-MHz ($32\,\mathrm{km\,s^{-1}}$) resolution. The shaded region indicates the expected frequency range for CO (3–2) emission from the GRB 090423 host galaxy, assuming a 1σ error range on the optical/near-infrared redshift. The spectra shown span $10\,000\,\mathrm{km\,s^{-1}}$ in velocity space and represent only 35 per cent of our total observed frequency range. The effect of primary beam attenuation on channel noise at the line emitter location is clearly visible.

4 RADIO SOURCES IN THE GRB FIELD

4.1 Continuum sources

We quantify the number density of continuum sources in our field, considering a circular region extending from the pointing centre to the radius at which primary beam attenuation limits sensitivity to 40 per cent of its maximum value (47 arcsec), yielding a survey area of $5.4 \times 10^{-4}\,\mathrm{deg^{-2}}$. We detect a single unresolved 5σ source in our 4-GHz-bandwidth continuum image, with a peak flux $S_{8\mathrm{mm}} = 15.9 \pm 3.2$ μJy, determined by fitting a Gaussian point source to the image data. The source lies 33 arcsec to the south-east of the GRB host galaxy. Two other features in the continuum map occur at 3σ relative to the local noise level.

In each case, several faint galaxies are visible at the source location in available deep *J*- and *H*-band imaging of the field (see Section 4.2), but the large beam size of the ATCA at 39 GHz prevents secure identification of the correct near-infrared counterpart (if any) or determination of an accurate redshift. None of the three continuum sources shows evidence for strong line emission in the frequency range observed.

4.2 Molecular line emitter

In principle, we are sensitive to any emission-line source appearing in the telescope primary beam and in our 36–40 GHz frequency range. In practice, this region of the spectrum is largely devoid of significant lines from Galactic or low-redshift sources (Lovas, Johnson & Snyder 1979). The only strong features seen from

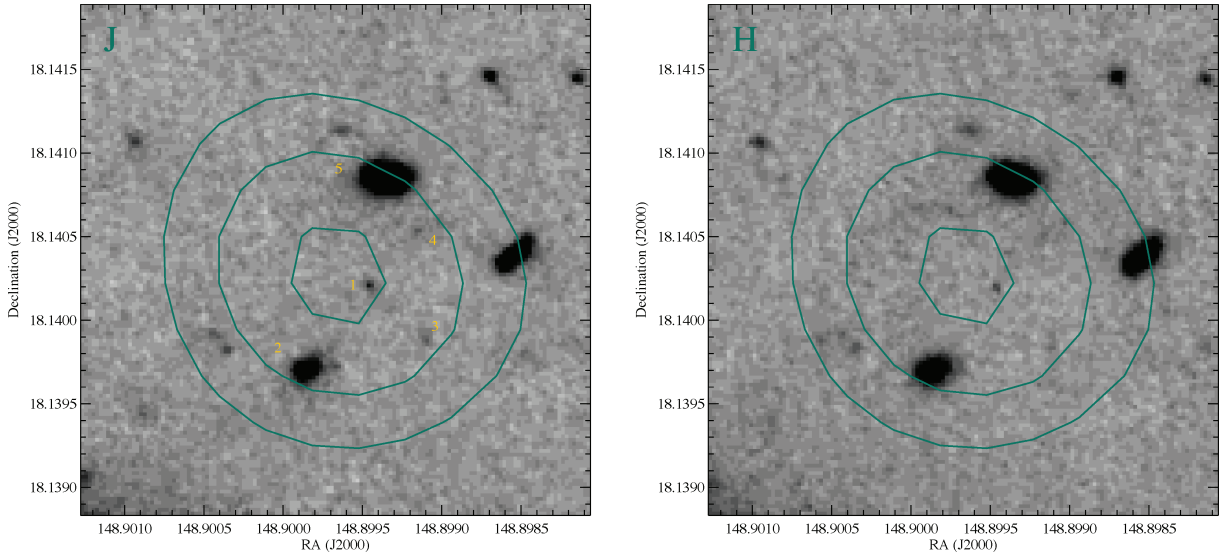

Figure 2. Deep near-infrared imaging in the *F125W* (*J*) band and *F160W* (*H*) band, overlaid with contours showing the spatial position of CO line emission, integrated across the 22-MHz width of the line emission. Contours mark 5σ, 7.5σ and 10σ levels relative to the noise in the line-integrated image. Images are 12 arcsec on a side and oriented with north uppermost. As discussed in Section 4.2, the synthesized beam of our observations at this frequency is 8.00×6.45 arcsec^2 and the pointing is accurate to approximately half a beam (roughly corresponding to the second contour). It is apparent that a number of plausible counterparts exist for the line emitter with the five best-detected labelled in the *J*-band image.

Galactic sources in this frequency range (i.e. emission lines without comparable-strength neighbouring lines) are high-order transitions in methanol masers, which are usually highly polarized and associated with high-mass star formation regions.

There are only three credible extragalactic interpretations of an emission line occurring at these high frequencies. We are sensitive to CO (1–0) line emission occurring at $z = 2.05 \pm 0.15$, CO (2–1) at $z = 5.10 \pm 0.30$ and CO (3–2) at $z = 8.15 \pm 0.45$.

The data cube obtained contains spectral information for any source lying within the primary beam of the ATCA. We rigorously inspected our data cube for emission-line candidates lying within 47 arcsec of the pointing (and hence phase) centre. As in the case of the GRB host galaxy, we consider the data rebinned in frequency on scales ranging from 16 to 126 km s^{-1} per spectral resolution element, searching both for particularly narrow-line emission and for weaker but broader emission lines. Clear detections at the same spatial location in three or more adjacent channels were required to identify an emission-line candidate. While pattern noise in the reduced images often creates strong peaks in the noise distribution, these are limited to one spectral channel, and noise peaks in adjacent channels appear spatially offset from one another.

We identify a single strong emission-line source in our spectral data cube, centred at 37.164 GHz as shown in Fig. 1. The best-fitting Gaussian line profile has a peak flux of 0.58 ± 0.12 mJy and a velocity FWHM of 96 km s^{-1}, yielding an integrated line flux $S_{\rm CO}\Delta v = 0.059 \pm 0.012$ Jy km s^{-1}, accounting for primary beam attenuation.[2] The line flux is not significantly polarized (although we note that at this low signal-to-noise ratio, there is large flux uncertainty in each polarization). The source, located at $09^{\rm h}55^{\rm m}35\overset{\rm s}{.}96+18^\circ08'24\overset{''}{.}7$, is not detected in 8-mm continuum emission.

As discussed above, three plausible redshifts exist for this source: $z = 2.10$, 5.20 and 8.31, corresponding to the first three rotational transitions of the carbon monoxide molecule. Due to the offset between redshift, luminosity distance and intrinsic line flux for these three transitions, our observations reach comparable mass sensitivities in all three lines: 1.0, 1.1 and 0.98×10^{10} M$_\odot$ in molecular gas, respectively (assuming $M_{\rm gas}/L'_{\rm CO} = 0.8$ as discussed in Section 3).

Since the galaxy almost certainly does not fill our 7.8×6.3 arcsec^2 beam, a detailed calculation of the dynamical mass is not possible with the current data, and, in fact, it is not clear whether the linewidth is actually diagnostic of ordered rotation in sources of this type. However, while the emission-line velocity width is narrow, it is consistent with the calculated gas mass if the molecular gas is distributed in a virialized disc 1 arcsec in diameter at $z = 8$ (0.6 arcsec at $z = 2$), seen close to face-on.

Given the hierarchical model for galaxy formation, and in the absence of additional information on large-scale structure in this field, our a priori most likely interpretation has to be that this is an intermediate-mass star-forming galaxy at $z = 2.10$. Such a galaxy would typically be easily detected in deep optical ($I \approx 24$ in similar mass examples; see Casey et al. 2009) and near-infrared data, although the presence of significant amounts of dust could lead to the absence of a counterpart (as is the case for submillimetre luminous galaxies). Higher redshift sources would typically be both fainter and bluer in the near-infrared.

In Fig. 2 we show existing deep near-infrared imaging of the region from *Hubble Space Telescope (HST)*/WFC3 (P.I. Tanvir, analysis in preparation). These data reached a limit of $J \sim 28.5$ (AB, 3σ) in a 1-arcsec aperture and was obtained in order to study the host galaxy of GRB 090423. Near-infrared data of this depth and quality are rare. Fig. 2 demonstrates the high-surface density of faint sources in such data and hence the difficulty of assigning an unambiguous counterpart to the line emitter. The ambiguity is further heightened by uncertainties in the pointing accuracy of the ATCA. At millimetre wavelengths, the telescope is used in a reference pointing mode, with a nearby calibrator (PKS 0953+254 in this case) used to check and refine the pointing solution once an hour throughout observations. Typical corrections at the end of each hour's observations were of the order of a few arcseconds and rarely exceeded half the size of the synthesized beam.

[2] It reduces the measured flux at this position to 42.5 per cent of its true value.

Given this uncertainty, there are five near-infrared sources, well detected in both bands, which may represent a counterpart for the line emission source, as well as a number of low-surface-brightness features at the noise level of the data. The $J - H$ colours of these sources are insufficient to provide a redshift estimate, although we note with interest that the faint unresolved point source closest to the centre of the line emission (marked '1' in Fig. 2) shows very blue near-infrared colours ($J = 27.4$, $J - H = -0.83 \pm 0.15$), a trait typical of high-redshift ($z > 5$) galaxies (e.g. Stanway, McMahon & Bunker 2005; Bouwens et al. 2010) and difficult to obtain for normal stellar populations at lower redshift.

Further data will be needed to unambiguously confirm the redshift of this source, and in the absence of such data, a tentative identification as CO (1–0) emission from a faint $z = 2.10$ starburst galaxy remains the most likely interpretation.

5 DISCUSSION

5.1 Constraints on the GRB host galaxy

A typical L* Lyman break galaxy at $z \approx 7$–8 is believed to have a stellar mass of a few $\times 10^9\,M_\odot$ (González et al. 2010; Labbé et al. 2010), although considerable uncertainties (primarily stellar population synthesis model used, metallicity, photometric uncertainty and the deblending of faint, confused sources) remain in this calculation. This is very comparable to the median stellar mass determined for GRB host galaxies at $z < 1.2$ ($1.3 \times 10^9\,M_\odot$; Svensson et al. 2010), and little evolution in this is seen to much higher redshifts either directly (Savaglio et al. 2009) or in semi-analytic simulations tuned to match the observed distribution at $z = 1$–6 (Chisari et al. 2010).

Our constraint on the mass of molecular gas in the host galaxy of GRB 090423 requires $M(H_2)$ to be within a factor of a few of this expected stellar mass for GRB hosts, suggesting either that the GRB host is less massive than those typical at lower redshift or that its star formation is already well advanced, i.e. that it must be at least a third of the way through its starburst process, assuming 100 per cent efficiency in the conversion of gas to stars.

This tight limit is sensitive to gas not only in the host galaxy itself, but in the $40 \times 30\,\mathrm{kpc}^2$ region encompassed by the synthesized beam of the observations. As a result the upper limit includes gas infalling on or recently ejected from a star-forming galaxy, and in any close neighbours. As such, it is somewhat surprising that a galaxy that is likely the progenitor of a much more massive low-redshift system has such a limited fuel supply available for later and ongoing star formation. While no data are currently available on the current star formation rate of this source, it is instructive to consider a crude model in which the host galaxy is typical of lower redshift GRB hosts (i.e. $M_* \approx 10^9\,M_\odot$) and star formation began at $z \approx 12$ (during the epoch of reionization), yielding a a stellar population age of 240 Myr and a continuous star formation rate of $4\,M_\odot\,\mathrm{yr}^{-1}$ [comparable to the median of $3.8\,M_\odot\,\mathrm{yr}^{-1}$ found in the GRB host sample of Svensson et al. (2010)]. In this model, the host galaxy will exhaust its fuel supply by $z \approx 5.7$ at the current rate of star formation. If the host is less massive or star formation began earlier (and hence the average star formation rate is lower), the star formation epoch may extend to lower redshifts.

We note that this conclusion is drawn from the assumption of an optically thick thermalized, metal-enriched gas and from a CO to H_2+He gas mass conversion factor that is calibrated on the most massive starbursts at intermediate redshifts. These assumptions may well be flawed on a number of levels. As mentioned in Section 3, the applicability of a simple conversion (widely known as the X-factor) from CO (1–0) luminosity to a gas mass has not been demonstrated at higher redshifts or in galaxies with sub-ULIRG star formation rates. The low M_{gas}/L'_{CO} ratio in ULIRGs is believed to arise from the presence of a galaxy-wide starburst in which the bulk of the interstellar medium is both dense and irradiated by star formation (Solomon et al. 1997). If the GRB host galaxy at $z \sim 8$ is, like those at intermediate times, similar in character to $z \sim 5$ Lyman break galaxies in terms of mass, metallicity and star formation rate, then it is interesting to note that such systems do indeed seem to be galaxy-wide starbursts with high specific star formation rates (Verma et al. 2007) and no evidence that the UV-luminous knots observed are merely super-starclusters embedded in a more massive, cooler medium (Davies et al. 2010; Stanway et al. 2010). While this may argue in favour of the ULIRG-like conversion ratio used in this paper, the low metallicity and comparitively low star formation rates of such sources may have the effect of increasing the ratio. This significant source of uncertainty must necessarily be addressed by later studies.

Although GRB 090423 is believed to be a Population II event and thus indicative of a metal-enriched star-forming population, the fraction of relatively pristine H_2 gas in the outer regions of a galaxy at early times is likely to be higher, particularly well outside the star-forming disc. Our observations cannot rule out the presence of a large reservoir of such gas, either in the host galaxy or in filaments surrounding it since this would likely not be reflected in the measured CO luminosity.

Similarly, the conversion assumes a known ratio of emission in the higher order rotational lines to that in the CO (1–0) fundamental transition. At high redshifts, the cosmic microwave background provides a minimum temperature for a typical galaxy, pushing the rotational excitation ladder of carbon monoxide to higher levels and hence reducing the measured flux in the lower excitation states. The effect of this is seen in the recent models of Obreschkow et al. (2009a), which indicate that the highest surface density of sources to a given flux limit is seen in CO (3–2) emission at low redshift and in CO (5–4) emission by $z = 5$. Future follow-up of this and similar sources with Atacama Large Millimetre Array (ALMA) (which, while having a more limited field of view, will access higher order CO transitions) may yield an indication of this effect and prove more successful in determining the precise source redshift and gas mass.

5.2 Large-scale structure at high redshifts

As mentioned in Section 4.2, our deep data cube probes cosmological volume in each of three redshift ranges. Considering the region in which our flux sensitivity is > 40 per cent of that at the pointing centre yields a field of view of $5.4 \times 10^{-4}\,\mathrm{deg}^{-2}$, while the 4-GHz bandwidth yields a line-of-sight depth of $\Delta z = 0.29$, 0.59 and 0.88 at $z = 2$, 5 and 8 respectively.

Given a single emission-line source (with redshift yet to be determined), we are able to place an upper limit on the surface density of CO-luminous galaxies in each of these redshift ranges. Our constraints are shown in Fig. 3, together with the predicted surface densities of sources with $L'_{CO} > 0.05\,\mathrm{Jy\,km\,s}^{-1}$ (i.e. to a flux limit matching our detection of a single possible line) determined from the *S-cubed* simulations of Obreschkow et al. (2009b). These analyse a conical section through the Millennium Simulation, applying a semi-analytic prescription to calculate the predicted CO rotation emission-line excitation ladder and H_2 gas properties associated

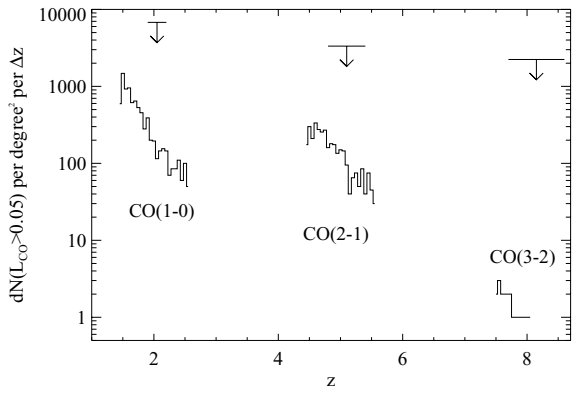

Figure 3. Our upper limit on the number density of line emission sources satisfying $L'_{\rm CO} > 0.05\,{\rm Jy\,km\,s^{-1}}$, given the velocity-integrated flux of our single detected line emitter (i.e. assuming that we detect 1 or fewer sources in each redshift range). Also shown are predicted number densities of sources satisfying the same constraint in each emission line from the semi-analytic models of Obreschkow et al. (2009b) as discussed in Section 5.2. Since these models are based on a section through the Millennium Simulation, they are subject to small number statistics in the predicted number densities, particularly at the highest redshifts.

with about 2.8×10^8 dark matter haloes.[3] As Fig. 3 demonstrates, very few $z = 8$ galaxies in the simulation would satisfy our flux selection limit in the CO (3–2) line (the simulation field of view at $z = 8$ is about $4 \times 4\,{\rm deg}^2$), and hence the uncertainty on the predicted number densities is dominated by small number statistics.

Interestingly, regardless of which line identification is considered most likely, our detection of a CO-emitting source is something of a surprise. Given these simulations, and in the absence of lensing, we might expect to have detected either a $z = 2.1$ CO (1–0) emission line or a $z = 5.2$ CO (2–1) emission line of this strength in one of 35 blind ATCA pointings. It is possible that one of the intermediate redshift galaxies visible in Fig. 2 is a lensing source, boosting the flux of a $z = 2$ or $z = 5$ background galaxy, or that we have chanced across rare large-scale structure at these redshifts.

The probability of a randomly selected pointing detecting a $z = 8$ galaxy in CO emission is considerably lower (approximately 1 in 2000). However, this field is not randomly selected. In the unlikely event that follow-up investigations confirm the very blue ($J - H = -0.8$) faint galaxy as a $z = 8$ near-infrared counterpart to the emission-line source, this field would host both a GRB and a more massive gas-rich source (separated by a projected distance of 200 kpc), representing a highly significant overdensity above the typical galaxy distribution at this redshift and suggesting that GRBs are indeed effective tracers of large-scale structure at high redshift. While constraints from a single GRB and associated field remain weak, such a detection might argue against the suppression of star formation in low-mass haloes seen in warm dark matter models, as discussed by Mesinger et al. (2005), which are expected to yield both fewer high-redshift GRBs and fewer star-forming galaxies associated with them.

Even by $z = 8$, the effects of cosmic variance can be significant. Iliev et al. (2010) have suggested a two order-of-magnitude variation in the density of 0.5-Mpc^3 regions at this redshift, based on large N-body simulations probing structure formation during reionization. Given the significant expenditure of telescope time necessary to obtain deep imaging suitable for exploring the $z \sim 8$ Universe, exploring underdense regions is likely to be both disappointing and uninformative. Following up GRB fields (should additional $z > 6$ bursts be identified) may well be the most efficient method for identifying the high density regions that are the sites for later massive galaxy and cluster formation.

[3] http://s-cubed.physics.ox.ac.uk/s3_sax/sky

6 CONCLUSIONS

We have observed the host galaxy of GRB 090423 and its immediate environs at radio frequencies (36.1–39.7 GHz), in order to search for molecular gas emission in the CO (3–2) line. Our main conclusions can be summarized as follows.

(i) No continuum source was seen at the GRB location in the multi-frequency synthesis image, allowing us to place an upper limit on the 37.9-GHz flux of this source of $S_{8\rm mm} = 9.3\,\mu$Jy (3σ, assuming the source is unresolved).

(ii) No line emission is detected from the GRB 090423 host galaxy. Applying standard conversion factors, we determine an upper limit on the molecular gas in this $z = 8.23$ source of $M(H_2) < 4.3 \times 10^9\,M_\odot$ (3σ).

(iii) This tight limit on the fuel for star formation suggests either that the GRB host is less massive than those seen at lower redshift or that its starburst is well advanced. We caution that this conclusion depends critically on the assumptions required to calculate gas masses, which are not yet well calibrated at high redshift.

(iv) We identify a single strong emission-line source in our data, centred at 37.164 GHz and 44 arcsec to the south-west of the GRB. The emission has a peak flux of 0.58 ± 0.12 mJy and a velocity FWHM of $96\,{\rm km\,s^{-1}}$. This corresponds to a molecular gas mass of 1.0, 1.1 or $0.98 \times 10^{10}\,M_\odot$ if we interpret the line as CO (1–0) at $z = 2.1$, CO (2–1) at $z = 5.2$ or CO (3–2) at $z = 8.3$, respectively. Efforts to identify and characterize a counterpart to this emission-line source are continuing.

ACKNOWLEDGMENTS

ERS gratefully acknowledges support from the UK Science and Technology Facilities council. Based on data obtained at the ATCA as part of programme C2153. The ATCA is part of the Australia Telescope which is funded by the Commonwealth of Australia for operation as a National Facility managed by CSIRO. The WFC3 data referenced in Section 4.2 are associated with *HST* Proposal 11189 and we thank the co-investigators of that project for kindly allowing us access to the data here. We would like to thank Mark Birkinshaw and Matt Lehnert for useful discussions during the preparation of this manuscript. We also thank Ben Humphries and Shari Breen for their assistance as Duty Astronomers during our observations.

NOTE ADDED IN PRESS

Flux limits given in Sections 2 and 3 are obtained from data that have been 'cleaned' using MIRIAD. Further inspection and consultation with ATCA staff suggests that a less vigorous cleaning strategy may be appropriate. This would result in a factor of 2 increase in the quoted flux and mass constraints, but has no substantive impact on our discussion or science conclusions.

REFERENCES

Aravena M. et al., 2008, A&A, 491, 173
Bouwens R. J. et al., 2010, ApJ, 708, L69
Campana S. et al., 2007, ApJ, 654, L17
Casey C. M. et al., 2009, MNRAS, 399, 121
Chisari N. E., Tissera P. B., Pellizza L. J., 2010, preprint (arXiv:1005.4036)
Coppin K. et al., 2010, MNRAS, 407, L103
Davies L. J. M., Bremer M. N., Stanway E. R., Birkinshaw M., Lehnert M. D., 2010, preprint (arXiv:1007.3989)
González V., Labbé I., Bouwens R. J., Illingworth G., Franx M., Kriek M., Brammer G. B., 2010, ApJ, 713, 115
Iliev I. T., Moore B., Gottloeber S., Yepes G., Hoffman Y., Mellema G., 2010, preprint (arXiv:1005.3139)
Kistler M. D., Yüksel H., Beacom J. F., Hopkins A. M., Wyithe J. S. B., 2009, ApJ, 705, L104
Labbé I. et al., 2010, ApJ, 708, L26
Lamb D. Q., Reichart D. E., 2000, ApJ, 536, 1
Lovas F. J., Johnson D. R., Snyder L. E., 1979, ApJS, 41, 451
McQuinn M. et al., 2009, Astro White Paper, 2010, 199
Maiolino R., Schneider R., Oliva E., Bianchi S., Ferrara A., Mannucci F., Pedani M., Roca Sogorb M., 2004, Nat, 431, 533
Mesinger A., Perna R., Haiman Z., 2005, ApJ, 623, 1
Mészáros P., Rees M. J., 2010, ApJ, 715, 967
Mo H. J., White S. D. M., 2002, MNRAS, 336, 112
Obreschkow D., Heywood I., Klöckner H.-R., Rawlings S., 2009a, ApJ, 702, 1321
Obreschkow D., Klöckner H.-R., Heywood I., Levrier F., Rawlings S., 2009b, ApJ, 703, 1890
Oesch P. A. et al., 2010, ApJ, 709, L21
Oke J. B., Gunn J. E., 1983, ApJ, 266, 713
Ruiz-Velasco A. E. et al., 2007, ApJ, 669, 1
Salvaterra R. et al., 2009, Nat, 461, 1258
Savaglio S., Glazebrook K., LeBorgne D., 2009, ApJ, 691, 182
Solomon P. M., Vanden Bout P. A., 2005, ARA&A, 43, 677
Solomon P. M., Downes D., Radford S. J. E., Barrett J. W., 1997, ApJ, 478, 144
Stanway E. R., McMahon R. G., Bunker A. J., 2005, MNRAS, 359, 1184
Stanway E. R., Bremer M. N., Davies L. J. M., Birkinshaw M., Douglas L. S., Lehnert M. D., 2008, ApJ, 687, L1
Stanway E. R., Bremer M. N., Davies L. J. M., Lehnert M. D., 2010, MNRAS, 407, L94
Stratta G., Maiolino R., Fiore F., D'Elia V., 2007, ApJ, 661, L9
Svensson K. M., Levan A. J., Tanvir N. R., Fruchter A. S., Strolger L.-G., 2010, MNRAS, 479
Tacconi L. J. et al., 2008, ApJ, 680, 246
Tanvir N. R. et al., 2004, MNRAS, 352, 1073
Tanvir N. R. et al., 2009, Nat, 461, 1254
Totani T., Kawai N., Kosugi G., Aoki K., Yamada T., Iye M., Ohta K., Hattori T., 2006, PASJ, 58, 485
Verma A., Lehnert M. D., Förster Schreiber N. M., Bremer M. N., Douglas L., 2007, MNRAS, 377, 1024
Wang F. Y., Dai Z. G., 2009, MNRAS, 400, L10
Wyithe J. S. B., Hopkins A. M., Kistler M. D., Yüksel H., Beacom J. F., 2010, MNRAS, 401, 2561

This paper has been typeset from a TEX/LATEX file prepared by the author.